LBL-22428
Preprint

Lawrence Berkeley Laboratory
UNIVERSITY OF CALIFORNIA

Materials & Molecular Research Division

Submitted to Journal of Chemical Physics

RADIATIVE DECAY LIFETIMES OF CH_2^-

M. Okumura, L.I. Yeh, D. Normand,
J.J. Van Den Biesen, S.W. Bustamente, Y.T. Lee,
T.J. Lee, N.C. Handy, and H.F. Schaefer III

October 1986

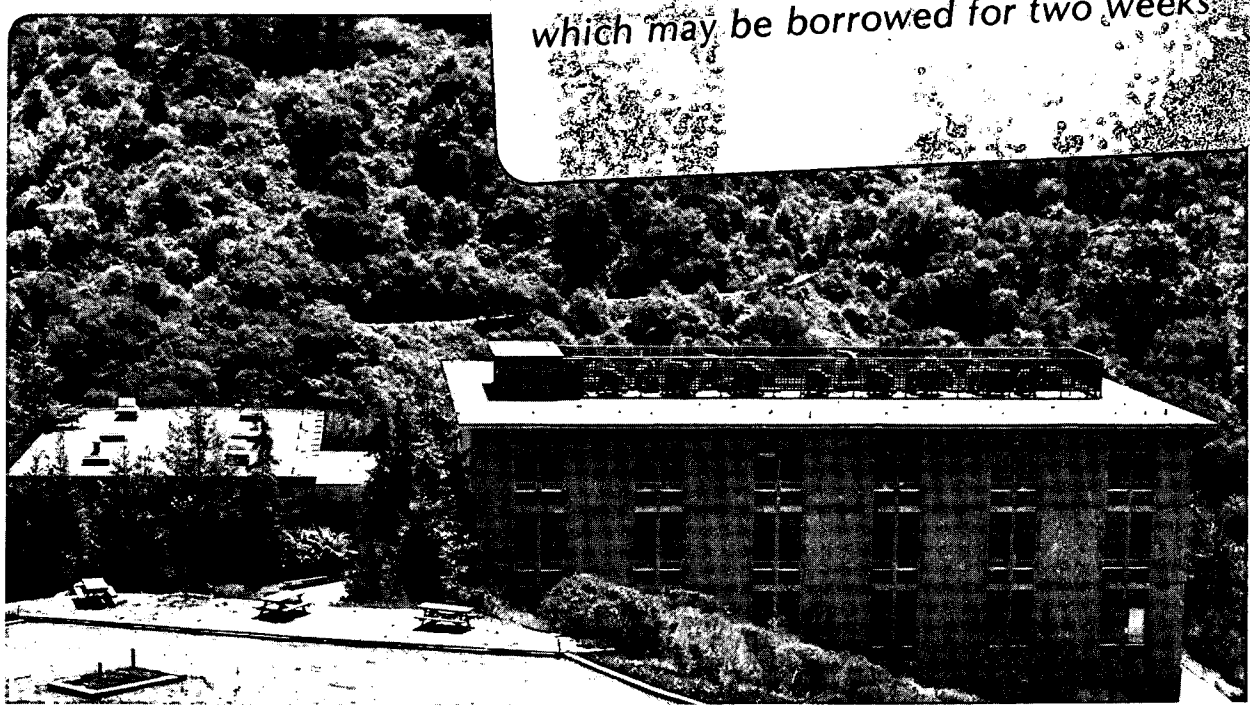

Prepared for the U.S. Department of Energy under Contract DE-AC03-76SF00098

DISCLAIMER

Radiative Decay Lifetimes of CH_2^-

M. Okumura, L. I. Yeh, D. Normand,[a]

J. J. H. Van Den Biesen[b], S. W. Bustamente[c] and Y. T. Lee

Materials and Molecular Research Division
Lawrence Berkeley Laboratory and
Department of Chemistry
University of California
Berkeley, California 94720

and

Timothy J. Lee, Nicholas C. Handy[d], and Henry F. Schaefer III

Materials and Molecular Research Division
Lawrence Berkeley Laboratory and
Department of Chemistry
University of California
Berkeley, California 94720

[a]Permanent address: C. E. N./Saclay, Dph. G/S. P. A. S., 91191, Gif-sur-Yvette, France.

[b]Permanent address: WAS 1414 Philips Research Laboratories, Postbox 8000, 5600 J. A. Eindhoven, Netherlands.

[c]Permanent address: Hughes Aircraft Corp., P.O. Box 2999, Torrence, CA 90509.

[d]Permanent address: University Chemical Laboratory, Lensfield Road, Cambridge, CB2 1EW, England.

Abstract

Recently the presence and radiative decay of vibrationally excited CH_2^-, generated in a hot cathode discharge of methane, was established by measuring the time dependent photodetachment from excited states of CH_2^- as it radiatively relaxed in a high vacuum ion trap. The time dependence of the photdetachment was found to be consistent with an electron affinity of 5250 cm^{-1} (0.65 ev) for ground state $\tilde{X}\ ^3B_1$ methylene. The radiative decay lifetimes of the first three excited bending vibrations of CH_2^- were also tentatively assigned. Here, we report a more refined analysis of the experimental data along with theoretical ab initio determinations of the radiative decay lifetimes of the first 4 excited bending vibrational levels of CH_2^-. There is some discrepancy between the ab initio values (431, 207,118 and 68 milliseconds for the v_2 = 1, 2, 3 and 4 levels respectively) and the experimental values (525, 70 and 14 milliseconds - for v_2 = 1, 2 and 3 respectively) for v_2 = 2 and 3. Possible reasons for this discrepancy are discussed but none of the alternatives are entirely satisfactory.

I. Introduction

Recently we presented[1] preliminary results for the determination of the radiative decay lifetimes of vibrationally excited CH_2^-. The main purpose of the original work was to demonstrate the existence of vibrationally excited ($v_2 \neq 0$) CH_2^- when created in a discharge. Hot bands are a potential problem in the photoelectron and photodetachment spectroscopy of negative ions created by discharge, sputter and other high temperature ion sources.[2,3] The interpretation of the first photoelectron spectrum of the methylene anion proved to be particularly difficult[4] because the standard techniques used to identify hot bands failed to do so. It is now well established,[1,5,6] though, that hot bands were present in the photoelectron spectrum as first suggested by Harding and Goddard.[7]

Using a radio frequency (rf) ion trap at very low pressures, we were able to trap CH_2^- ions without collisions, and measured the radiative decay of the hot band signal as a function of trapping time. The decay rates of individual v_2 levels were obtained from a tentative fit of the data. In this paper we examine more carefully the radiative lifetimes of the v_2 bending vibrations of $\tilde{X}\ ^2B_1$ CH_2^-. We present both *ab initio* calculations of the v_2 = 1, 2, 3, and 4 lifetimes and a more refined analysis of the data, including additional data not reported earlier.

Leopold *et al.* have presented photoelectron spectra of "cold" CH_2^- created in a flowing afterglow. Their work, along with a semi-rigid bender analysis by Sears and Bunker, provides a clear description of this anion. The $\tilde{X}\ ^2B_1$ state has a bond angle of 103°, and a barrier to linearity of approximately 10,000 cm^{-1}. The electron affinity of $\tilde{X}\ ^3B_1$ CH_2 is 0.645 ± 0.008 eV, in excellent agreement with predictions of *ab initio* calculations. The C-H bond lengths of these two states are nearly identical, but the triplet CH_2 radical

is quasi-linear, with a bond angle of 134.8°, and a barrier to linearity of only 1940 cm^{-1}. As a result, the Franck-Condon overlap for $\Delta v_2 = 0$ transitions is small, and the photoelectron spectrum is characterized by a progression in the v_2 bending transition. In contrast, the low lying $\tilde{a}\ ^1A_1$ state of the neutral is nearly identical in geometry to the anion, and it contributes a single large peak at $\Delta v_2 = 0$. This state lies 3165 cm^{-1} above the ground state.

Bunker and Langhoff[8] have presented transition moment matrix elements of vibrational transitions, for $\tilde{X}\ ^3B_1CH_2$ and $\tilde{a}\ ^1A_1CH_2$. These were determined from ab initio electronic structure calculations coupled with semi-rigid-bender (SRB) vibrational wavefunctions. In fact we used[1] the $\tilde{a}\ ^1A_1CH_2$ data in the comparison of the radiative decay lifetimes of $\tilde{X}\ ^2B_1\ CH_2^-$ and $\tilde{a}\ ^1A_1CH_2$. Although these states have similar geometries and bending potentials, their dipole moments differ considerably and so may the dipole moment surfaces. A comparison of the neutral and anion lifetimes can be of only limited usefulness.

Because the CH_2^- bending vibration is a large amplitude motion, a large part of the potential and dipole moment surfaces are sampled. Such calculations are relatively difficult, and have not been systematically investigated.

It is a well known fact that highly accurate ab initio predictions for anions are difficult, requiring extremely large basis sets coupled with highly correlated wavefunctions. In a recent study Lee and Schaefer[9] demonstrated that even at the self-consistent-field (SCF) level of theory rather large basis sets are necessary in order to "converge" many molecular properties. Thus, it was necessary first to determine the size and type (i.e., how many s, p and d functions) of basis set needed at the configuration interaction (CI)

level of theory. Though it is not the purpose of this paper to detail the results of the basis set study as that will be done in a later publication,[10] an indication of the sensitivity to the basis of several geometrical properties will be given.

Of course many studies of polyatomic anionic species have involved the use of correlated wavefunctions, but to the best of our knowledge, none have explicitly investigated the basis set dependence on all the properties of interest here, namely geometrical structure, surface shape and most importantly, the dipole moment surface. It is noteworthy that Werner, Rosmus and coworkers[11-13] have theoretically investigated OH^-, C_2^-, NH^- and CH^- and Botschwina[14-16] has studied CN^-, CCH^- and NH_2^-. Werner, Rosmus and Reinsch[11] demonstrated the need of a multi-configuration self-consistent-field (MCSCF) reference wavefunction for diatomics, but this undoubtedly is due in large part to the inadequate description of the dissociation process which plague restricted Hartree-Fock (RHF) SCF wavefunctions. We believe that for the type of molecular motion which is being studied here, specifically the bending mode in a symmetric, non-linear triatomic, the SCF wavefunction should give a good zeroth order description. The one possible exception to this may be when the HCH angle is very small (i.e., $CH_2^- \rightarrow C^- + H_2$). However, we did not see any evidence for the deterioration of the single configuration reference function as the bond angle decreased. Further support for this argument can be found in a recent study on the effects of triple and quadruple excitations on the harmonic vibrational frequencies of several molecules,[17] where it was found that these higher excitations contributed very little to bending harmonic frequencies.

In Botschwina's study[14] of NH_2^- he did not include the dipole moment or the infrared (IR) intensities. Also, though the final basis is rather

large,[11-16] only one basis set is used for CCH^- and NH_2^- and two for CN^-. Thus it is difficult to deduce any basis set dependencies.

It is also of interest to note the recent work of Adler-Golden, Langhoff, Bauschlicher and Carney (ALBC) on the ozone molecule.[18] Although O_3 is not an anion, ALBC's work is relevant because of their success in reproducing the experimental IR intensities, which depend upon the same transition moment matrix elements as do vibrational radiative decay lifetimes. Using a complete active space self-consistent-field (CASSCF) wavefunction to compute the dipole moment function and an experimental potential function, ALBC obtain IR intensities in reasonable quantitative agreement with experiment for fundamentals, hot bands and combination bands. ALBC computed the energy and dipole moment for more than 200 points of the CASSCF Born-Oppenheimer potential energy surface and then used a variational approach to solve for the vibrational wavefunctions.

The goal of the present study is to determine the radiative decay lifetimes of the bending mode in CH_2^- with qualitative and semi-quantitative accuracy. Since it is believed that the ν_2 fundamental and combinations thereof are reasonably far removed from the ν_1 and ν_3 fundamentals (and combinations) it is a reasonable approximation to ignore their coupling. Therefore, the SRB model Hamiltonian[19] of Bunker and Landsberg is a useful method for obtaining the bending vibrational wavefunctions. Equally important is the existence of an empirically derived SRB potential function[20,21] for CH_2^-. This will enable the purely <u>ab initio</u> radiative decay lifetimes to be compared with those obtained with the empirical potential and the <u>ab initio</u> dipole moment function.

The reader should realize that CH_2^- is a Renner-Teller molecule like the carefully studied NH_2 molecule. The barrier to linearity is on the order of

10,000 cm^{-1}, and in this paper we are only considering vibrational levels up to approximately 5,000 cm^{-1} above the lower state ($^2B_1$) minimum. Furthermore we are also only considering J=0 states. Experimental evidence cannot distinguish between the different rotational effects and the results presented here represent a Boltzman average of these effects. With these restrictions the theoretical analysis is considerably simplified because if $J \neq 0$, a correct theory must involve both the $^2B_1$ and $^2A_1$ surfaces. However, if the similarity between CH_2^- and NH_2 is realized then one would expect the Renner-Teller couplings to be small for small v quantum numbers and $J \neq 0$.

The details of the experiment and the analysis of the data are presented in Section II. In Section III the ab initio methods and results are presented. Finally, in Section IV we discuss and relate the theoretical and experimental results from the two previous sections.

II. Experiment

A. Experimental Details

Radiative decay rates of vibrationally excited ions can be measured, free of collisions, using the ion trapping technique. This technique is especially suitable for excited states with lifetimes longer than 1 ms, which are difficult to measure by more conventional techniques. A problem with ion trapping experiments lies in the low densities of ions that can be trapped, making it difficult to directly observe emitted photons. Instead, many such measurements probe the excited state population as a function of trapping time by other means. For negative ions, one can measure the photodetachment signal using photons with energies less than the electron binding energy for the ground state and greater than that for the excited states. Electrons will be detached only from ions in excited states. At a given trapping time, the depletion caused by a laser pulse will provide a measure of the population of all those excited states which are bound by energies less than the photon energy. The relative signal from each state will depend upon the cross-section for photodetachment.

The experimental apparatus, shown schematically in Figure 1, is described in detail elsewhere.[22,23] The machine is a tandem mass spectrometer, with a radio frequency (rf) octopole ion trap. A magnet mass filter first mass selects a beam of CH_2^- ions. These ions are then injected into the octopole ion trap, where they are stored for some trapping time. The population of excited state ions is then probed with a pulsed laser tuned to a desired photon frequency. The remaining ions are released, mass analyzed, and counted. An identical cycle is repeated, with the laser off. The relative difference between the two cycles gives the average laser-induced depletion at that trapping time. We obtain the radiative decay by incrementing the

trapping time and measuring the remaining excited state populations.

The methylene anions were created in a duoplasmatron source, in a discharge of 30 to 300 millitorr of 99.999% pure methane (Matheson ultra-high purity), with typical discharge currents of 1-2 mA. Like the Branscomb source used in the early photelectron experiments on CH_2^-, this source was a hot cathode discharge. To help confine the plasma, an external magnetic field was applied and an intermediate electrode was placed between the anode and cathode. A tungsten rod ran down the center of the source, as previous work has shown that this aided in negative ion formation. The ions were extracted from the source, accelerated to approximately 350 eV, and mass-selected with a 20 cm raidus sector magnet. An electrostatic quadrupole field deflected the ion beam 90°. The ions were then focused and decelerated to approximately 0.5 eV upon entering the trap.

We trapped the ions inside a 50 cm long rf octopole ion guide. The octopole was constructed of eight 50 cm long rods, 0.3 cm in diameter, symmetrically placed on a circle of 1.25 cm diameter. By applying opposite phases of rf to alternate rods, an oscillating octopole field was created, which effectively trapped the ion motion transverse to the axis of the trap. The ions were confined inside the ocotopole by the dc potentials of lens elements on either end of the octopole. The pressure in the trap region was appoximately 3×10^{-9} torr.

For 0.5 ms to 1 ms, the lens element at the entrance of the trap was kept at a potential to focus the ions into the trap. The lens potential was then raised to 10 eV above the d.c. bias of the trap, confining the ions in the trap and stopping further ions from entering. After a delay interval, during which excited ions would decay, the laser was fired into the trap. The ions were then released from the trap, mass analyzed, and detected with a ceratron

electron multipler. The data cycle was repeated, with the laser off. After averaging many pairs of cycles, the difference gave the average depletion at that trapping time. Decay curves were generated by incrementing the trapping time and measuring the fractional depletion.

We used a simple optical parametric oscillator (OPO) as our source for tunable infrared radiation. The OPO was a $LiNbO_3$ crystal in a simple cavity with no grating, pumped by the far field of a Quanta Ray Hd:YAG laser. We operated the laser at degeneracy (4700 cm^{-1}), where the linewidth of 200 cm^{-1} and pulse energy of 10 to 18 mJ were anomalously large. The laser repetition rate was kept at a constant 10 Hz. For scans with delays greater than 40 ms, the OPO pulse was selected with a shutter.

B. Results

The decay of the photodetachment signal at 4700 cm^{-1} is shown in Figure 2. Since our preliminary report,[1] we have obtained additional data recorded at the short times. The decay is clearly not a single exponential. In contrast, at a photon energy of 9394 cm^{-1}, approximately 67% of the ions are photodetached at all trapping times. The power dependence, shown in Figure 3, reveals at least three different components, two of which are saturated. After 30 ms, the state with the largest cross-section has disappeared.

The photon energy of 4700 cm^{-1} is 500 cm^{-1} (0.06 eV) less than the electron binding energy. The multiple exponential decay arises because all states with more than 500 cm^{-1} of internal energy can be photodetached. Assuming a temperature of 2500°K, derived from the photoelectron spectra by Sears and Bunker, the relative v_2 populations are 53%, 25%, 12%, 6% and 3% for v_2 = 0 through 4. The contribution to the photodetachment signal from each v_2 state depends upon the Franck-Condon factors as well as the number of final v_2

states accessible. The large change in the equilibrium bond angle and the bending potential causes the oscillator strength to be spread over several Δv_2 bands. The higher v_2 levels have more detachment channels available, and thus have larger cross sections at this photon energy.

The problem of cascading decays of an N-level system is an elementary problem of formal kinetics, for which the set of first order differential equations can be solved analytically. The solution requires initial populations, all decay rates A_{ij} (i.e., the Einstein coefficients for the transition from state i to j), and, for our data, relative photodetachment cross-sections σ_i. A unique fit of our data with such a large number of parameters is impossible, but the solution can be reduced to a simple sum of exponentials

$$Y(t) = \sum_{i=1}^{N} Y_i e^{-t/\tau_i} \quad (1)$$

where τ_i is the radiative decay lifetime of the ith level, and the effective pre-exponential factor Y_i is a function of the initial populations, the A_{ij}'s, and the photodetachment cross-sections. The data were fit to equation (1) using the τ_i's and the Y_i's as parameters.

The data were fit by a weighted nonlinear least squares to the sum of exponentials. Such a fit is notoriously difficult, especially if the decay rates are similar. We fit the data to a sum of three exponentials, and obtained lifetimes of 14^{+7}_{-7} ms, 70^{+50}_{-40} ms, and $524^{+\infty}_{-280}$ ms as reported (with the pre-exponential factors) in Table I. In general, the most reliable fits require data over a time span covering two lifetimes. The large uncertainty in the longest lifetime stems from the lack of data beyond 500 ms. A biexponential decay mechanism, yielding lifetimes of 20 ms and 296 ms, gave a

significantly poorer fit. The signal to noise was too poor to yield a unique fit to a four exponential model.

III. Theory

A. Theoretical Approach

All of the basis sets employed in this study embody the same starting point which is a [7s4p/3s] contraction of the (12s7p/6s) primitive sets of van Duijneveldt[24] for C and H, respectively. The contraction scheme used allows maximum flexibility in the valence region. A set of diffuse s and p functions ($\alpha_s(C) = 0.039906$, $\alpha_p(C) = 0.030237$) was added to the C sp basis and one set of diffuse s functions was added to the H basis ($\alpha_s(H) = 0.030155$). The smallest basis investigated contained two sets of polarization functions ($\alpha_d(C) = 1.5$ and 0.35; $\alpha_p(H) = 1.4$ and 0.25) on both C and H. This basis is designated [8s5p2d/4s2p] and is labeled TZ + diffuse + 2P as it was previously.[9] The contraction coefficients are also listed in Ref. 9. The second basis investigated had another set of diffuse sp functions added ($\alpha_s(C) = 0.015545$; $\alpha_p(C) = 0.011808$; $\alpha_s(H) = 0.010310$) and is labeled TZ + 2 diffuse + 2P. The third basis set can be designated TZ + diffuse + 3P' where now there are three sets of polarization functions on C ($\alpha_d(C) = 2.25$, 0.75, 0.25). Later it was found preferable to incorporate a set of more diffuse polarization functions into the C basis and so the TZ + diffuse + 3P basis consists of $\alpha_d(C) = 0.75$, 0.25, 0.083 for the carbon d functions. The final two bases were arrived at by adding yet another set of polarization functions to the carbon atomic basis. The basis labeled TZ + diffuse + 4P' has an additional C d-function with an exponent $\alpha_d = 2.25$ whereas the basis labeled TZ + diffuse + 4p has a more diffuse polarization function, $\alpha_d = 0.028$. The CI's included all configurations resulting from single and double replacements from the SCF reference wavefunction and hence are classified CISD. All CISD calculations were carried out with the shape-driven graphical unitary group approach CI method[25] and geometry optimizations used analytic CI gradient

techniques.[26,27] The CI dipole moment was evaluated with respect to the center of mass as an energy derivative.[28,29] It is worthy of noting that we support the authors of references 28 and 29 in their view that the dipole moment should be calculated as an energy derivative rather than an expectation value; the reason being that the extra term which occurs (the non Hellmann-Feynmann term) can be argued to be the correction of the CI wavefunction towards its MCSCF wavefunction.[27]

To give an idea of the basis set dependence Table II contains the CISD equilibrium geometry, and Table III gives the CISD dipole moment of CH_2^- for several basis sets. The results depicted in Tables II and III demonstrate the need of very diffuse polarization functions for anions at the CISD level of theory. This is especially true for the dipole moment where the TZ + diffuse + 3P' value (1.97D) is reduced to 1.72D with the TZ + diffuse + 3P basis set. Since the TZ + diffuse + 4P dipole moment is only 0.03D less than the TZ + diffuse + 3P value, the dipole moment function was determined initially with the TZ + diffuse + 3P basis, and later with the TZ + diffuse + 4P basis set.

In the SRB model[19] the effective bending potential and the bond length as a function of the supplement to the bond angle are required. The supplement is defined as $\rho = \pi - \alpha$ where α is the bond angle. The dipole moment function must also be a function of ρ . Therefore, the procedure we used was to optimize the C-H bond length (i.e., until $\partial E_{CI}/\partial r_{C-H} \cong 0$) at specific bond angles. The potential, bond length and dipole moment were then fit to a Taylor series expansion about linearity (at linearity $\rho = 0$). Because of the symmetry about linearity, only even powers of ρ appear in the potential and bond length functions and only odd powers of ρ appear in the dipole moment function. These functions (derived from the TZ + diffuse + 3P basis) are given in equations (2) through (4) with the units being cm^{-1}, A and D

respectively.

$$V(\rho) = -13951\ \rho^2 + 6733.1\ \rho^4 - 1555.7\ \rho^6 + 238.95\ \rho^8 - 16.101\ \rho^{10} \qquad (2)$$

$$r_{C-H}(\rho) = 1.081844 + 0.0230140\ \rho^2 - 0.000506\ \rho^4 \qquad (3)$$

$$\mu(\rho) = 3.033421\ \rho - 1.914737\ \rho^3 + 0.893442\ \rho^5 - 0.295384\ \rho^7 + 0.062339\ \rho^9 - 0.007390\ \rho^{11} + 0.000372\ \rho^{13} \qquad (4)$$

The potential and dipole moment functions were least squares fit from 18 points with α, the bond angle, ranging from 60° to 148°. The bond length function used only 13 points even though the bond was optimized for each angle α. Only 13 points were used here in order to minimize the variance of the fit. However, the bending energy levels as well as the transition moment matrix elements were quite insensitive to the bond length function used as long as it had the form of equation (3). These functions are shown in Figures 4-6. Also depicted in Figures 4 and 5 are the potential and dipole moment functions obtained with the TZ + diffuse + 4P basis. These calculations were performed at the TZ + diffuse + 3P geometries. The explicit forms of the functions are

$$V(\rho) = -14042\rho^2 + 6870.5\rho^4 - 1637.08\rho^6 + 259.97\rho^8 - 18.050\rho^{10} \qquad (5)$$

$$\mu(\rho) = 3.336752\rho - 2.715518\rho^3 + 1.748393\rho^5 - 0.793873\rho^7 + 0.225337\rho^9 - 0.035182\rho^{11} + 0.00228163\rho^{13} \quad . \qquad (6)$$

We did not consider asymmetric geometries for the following reasons. As noted previously, Bunker and Langhoff[8] have reported transition moment matrix elements for $\tilde{a}\ ^1A_1$ CH_2 using an empirically derived SRB potential with an ab initio dipole moment function. These were used by us previously[8] to determine the radiative decay lifetimes of the $v_2 = 1$, 2 and 3 states. Their dipole moment function has the form[8]

$$\mu_b = \rho \sin(c\rho) + q \sin^2(c\rho) + \mu'_a S_1 \tag{7}$$

and

$$\mu_a = \mu'_a S_3 \tag{8}$$

where $S_1 = \Delta r_i = r_i - r_e$. Equation (8) deals with asymmetric geometries and as noted we did not consider these. The last term in equation (7) allows for the change in the dipole moment with respect to changes in the bond length, and hence has more flexibility than our functional form. However, if this term is neglected the radiative decay lifetimes of $\tilde{a}\ ^1A_1$ CH_2 change by only +3, +1 and -4 milliseconds for the $v_2 = 1$, 2 and 3 levels respectively. Thus we were not compelled to incorporate a like term into the CH_2^- dipole moment function.

We also found it difficult to use the functional form of equation (7). We found it much easier to use a Taylor series expansion due to the shape of the dipole curve for CH_2^-. Figure 5 has a plot of the CISD dipole curves obtained from the TZ + diffuse + 3P basis and TZ + diffuse + 4P basis sets.

B. Radiative Decay Lifetimes

The determination of a radiative decay lifetime is rather straightforward and has been briefly reviewed by McKellar[5] and coworkers. The radiative decay

lifetime of the $v_2 = i$ vibrational state is given by

$$\tau_i = 1/\Sigma_j A_{ij} \tag{9}$$

where the Einstein A_{ij} coefficient is given by

$$A_{ij}/s^{-1} = \frac{64\pi^4}{3hc^3} (\omega_{ij}/cm^{-1})^3 \, |\langle i|\mu/D|j\rangle|^2 \tag{10}$$

$$= 3.14 \times 10^{-7} \, (\omega_{ij}/cm^{-1})^3 |\langle i|\mu/D|j\rangle|^2 \tag{11}$$

Here ω_{ij} is the difference of the vibrational levels $|i\rangle$ and $|j\rangle$, where $|j\rangle$ are the vibrational levels below $|i\rangle$. In the model used here the $|i\rangle$ and $|j\rangle$ are the SRB wavefunctions.

Table IV contains the experimentally determined radiative decay lifetimes, and the purely ab initio radiative decay lifetimes along with those obtained with the two SRB potentials of Sears and Bunker[20,21] coupled with the ab initio dipole moment function. As can be seen, there are not large differences between the sets of values. The results of Table IV indicate that the ab initio potential function is quite adequate and that the radiative decay lifetimes are very sensitive to the dipole moment function. Further support for the high quality of the ab initio potential is presented in Table V where the SRB vibrational energy levels for the various potential functions are given. The theoretical potentials agree with the empirically derived potentials reasonably well, especially in the lower levels.

The transition moment matrix elements and Einstein A coefficients used in determining the radiative decay lifetimes are listed in Tables VI and VII respectively. As is expected, the absolute value of the transition moment

matrix elements is largest for adjacent vibrational levels.

Not quite so easily predicted is the relationship of the Einstein A coefficients with Δv_2. For the i=3, 4 levels the Einstein A_{ij} coefficient is largest for $\Delta v_2 = 2$. Also interesting to note is that although the radiative decay lifetimes derived from the empirical potentials are very similar, the individual Einstein A coefficients are somewhat different and in fact the most recent potential[25] agrees much better with the ab initio results.

One way of testing the qualitative reliability of the theoretical decay lifetimes would be to determine the τ_1 lifetimes incorporating the double harmonic approximation (i.e., using mechanical and electrical harmonicity which means truncating the potential at quadratic terms and the dipole moment function at linear terms.) Harmonic vibrational frequency and IR intensity determinations for small molecules are becoming quite common, even at the CISD level of theory. Using the TZ + diffuse + 3D basis we obtain $\omega_1 = 2782\ cm^{-1}$, $\omega_2 = 1314\ cm^{-1}$ and $\omega_3 = 2841\ cm^{-1}$ with the corresponding IR intensities being 633 km/mole, 12 km/mole and 363 km/mole respectively. Using the ab initio dipole derivatives we determine the radiative decay lifetime of the first excited vibrational state to be τ_1 = 1.6 ms, 385 ms and 2.7 ms for the v_1, v_2 and v_3 modes respectively. The v_2 value is qualitatively similar to the value obtained with the SRB bending wave functions with this basis, 574 ms.

IV. Discussion

There are few calculations of vibrational intensities or lifetimes for polyatomic ions whose accuracy can be verified by experiment. Theoretical values of the v = 1 lifetime of CH^- agree to within 10% of the experimental value obtained in our laboratory, but the strong CH bond means that CH^- can be approximated by a harmonic oscillator quite reliably. A method such as the semi-rigid bender model used here should be more accurate than using the harmonic oscillator approximation.

The results of the current fit to three exponentials are similar to the previous results. We have initially assigned the three observed decays of 525, 70, and 14 ms to v_2 = 1, 2, and 3 respectively. The longest lifetime, 525 ms, agrees reasonably well with our theoretical v_2 = 1 lifetime of 431 ms. The latter is the most reliable of the theoretical lifetimes. The experimental values for the v_2 = 2, and v_2 = 3, (70 ms and 14 ms), however, are significantly smaller than the theoretical values of 207 ms and 108 ms. Thus, the lifetimes obtained from a fit with a three exponential model do not agree with theory.

The five- to seven-fold decrease in the experimental lifetimes with vibrational quantum number, however, seems anomalously large. The theoretical lifetimes decrease by only a factor of about two for each additional quantum in the bending mode. It is quite possible that an additional component with an intermediate lifetime is present but cannot be extracted from the data due to the signal-to-noise. Examination of the data reveals that there are not enough data points between 150 and 300 ms to preclude the existence of such a component.

The discrepancy between the results of the fit and theory indicate that four exponentials may be necessary. Although an unconstrained fit (eight

parameters) of the data to a sum of four exponentials does not yield a unique result, we can fit the data if we reduce the number of variables. The trend in the theoretical results suggest that we can assume a geometric progression for the four lifetimes. Therefore, we have performed several fits holding the ratio τ_i/τ_{i+1} constant. The range of lifetimes is large, and the lowest value of τ_i/τ_{i+1} that fits the data is 3.0, with lifetimes of 15 ms, 45 ms, 135 ms, and 405 ms. The $v_2 = 1$ lifetime agrees with the ab initio value, and the $v_2 = 2$ lifetime is somewhat closer to the theoretical result, but the two smaller lifetimes are still significantly less than theory. Therefore, the lifetimes extracted from the data using a four component model with constant τ_i/τ_{i+1} still do not completely agree with the theoretical results. Furthermore, the ratio $\tau_i/\tau_{i+1} = 2.5$ gives a fit one standard error worse than the best fit, with lifetimes of 19 ms, 47 ms, 118 ms, and 296 ms. Thus we cannot fit the data with the theoretical τ_i/τ_{i+1} of approximately two for a geometric progression of four lifetimes.

We have also tried to fit the experimentally observed curve in Fig 1, setting all the τ_i to the theoretical values, but have found that the data cannot be fit. The dashed curve in Fig. 2 is the result of such an attempt. Despite the ambiguities in fitting a multiple exponential decay, it is clear that the theoretical values for $v_2 = 1$ through 4 cannot reproduce the experimentally observed decay. The problem lies at the shortest times ($\tau < 30$ ms), where the experiemntal signal-to-noise is best, and the theory is the most uncertain.

The deviation of the dashed curve from the data suggest an alternative explanation for the disagreement. If the theoretical values for τ_i for i = 1, 2, and 3 are used, along with a fourth decay that is allowed to vary, the data can be fit, with $\tau_4 = 15$ ms. This result implies that the theoretical results

would be consistent with experiment if one postulates an alternative relaxation mechanism giving rise to a fast decay. We next consider possible sources for a fast decaying component.

The fast decay component could be the result of an experimental artifact; however, we have made a similar measurement of the excited state lifetimes of CH^- under almost identical experimental conditions, and observed lifetimes of 1.75 ms and 5.9 s,[23] but no evidence for a decay of 14 ms. For that system, we also found that collision-induced decay rates were much less than 1 s^{-1}. At the pressure used in this experiment, it is unlikely that collisions would be responsible for a process with a lifetime as fast as 14 ms. Furthermore, contamination from other species is probably not a problem. The mass resolution of the sector magnet is high: $\Delta M/M \approx 150$. The only contaminants would be isotopes of CH^-, but the lifetimes we observed for CH^- would not account for a 14 ms decay. We therefore believe that the 14 ms lifetime arises from the decay of an excited rovibrational state of $^2B_1$ CH_2^-.

If we extend the ab initio results to include the $v_2 = 5$ state a lifetime of 40 ms is obtained with the TZ + diffuse + 4P data. This value is somewhat longer than the observed lifetime. In addition, two objections might be raised to this possible explanation of the 15 ms experimental lifetime. First, even at a vibrational temperature of 2500 K, only 1.5% of the total population is expected to be in this level. Second, $v_2 = 5$ lies well above the threshold for electron detachment, and is therefore only metastable to electron loss.

We have thus far neglected contributions from the excited stretches $v_1 = 1$ and $v_3 = 1$. Based on isotope shifts and the Teller-Redlich rule, Leopold et al. estimate that the CH_2^- vibrational frequencies for ν_1 and ν_3 are 2580 cm^{-1} and 2635 cm^{-1} respectively. The theoretical harmonic values reported here

(2782 cm^{-1} and 2841 cm^{-1} respectively) are in reasonable agreement with these estimates, with both theoretical values being 7.8% higher. Bunker and Langhoff[8] have calculated the stretching transition moments for the neutal $\tilde{a}\ ^1A_1$ CH_2, in the double harmonic approximation. These yield radiative lifetimes of approximately 15 and 28 ms for ν_1 and ν_3 respectively. These lifetimes match the fast component we observed. However, performing the analogous calculation for CH_2^- (using the TZ + diffuse + 3P basis results) yields lifetimes of 1.6 ms and 2.7 ms respectively for the ν_1 and ν_3 modes. Also, these excited states are expected to have very small relative cross sections for photodetachment. The small change in the CH bond length (1.116 A for $^2B_1$ CH_2^- and 1.08 A for $^3B_1$ CH_2) results in very poor Franck Condon factors for transitions of the stretches with $\Delta v \neq 0$. No such transitions have been reported in any of the photoelectron spectra published to date. We observed that the fast component possessed a large relative cross section, with the transition seemingly saturated at the intensities used in our experiment. Thus, it is difficult to reconcile the observed cross section with the expected poor Franck-Condon overlap, and the estimated lifetimes of the stretches are not entirely consistent either.

In our calculation, we did not consider the possibility of a Fermi-resonance. Because the stretching modes have relatively large transition moments, the strong coupling of a stretching mode with a bending level $v_2 = n$ could greatly reduce the lifetime of the latter. The $v_2 = 1$ frequency of 2580 cm^{-1} estimated by Leopold et al. is very close to the $v_2 = 2$ level at 2584 cm^{-1} obtained from our best potential, but the actual frequencies are not known well enough.

Another possibility is that we are observing vibrational autodetachment of highly excited rovibrational states with energies above the electron

detachment threshold. The $v_2 = 4$ state, for instance, lies very close to the electron continuum. In order for the electron of a vibrationally excited anion to detach, the mechanism must involve a breakdown of the Born-Oppenheimer approximation. Very little is known about such vibrational autodetachment rates. Our fast component decays at a rate that is four to seven orders of magnitude slower than the NH^- rotational autodetachment rates observed by Neumark, Lykke, Andersen, and Lineberger,[30] and three orders of magnitude slower than the SF_6^- autodetachment rates.[31] These experiments are sensitive to fast processes, and cannot measure slower rates, whereas the experiment reported here can only measure long decays. Thus, long-lived atuodetaching states may have been present but unobserved in the earlier experiments. However, rovibrational states of CH_2^- that are metastable to detachment may not to be long-lived. There is a crossing of the CH_2 anion and neutral potential energy curves possibly near $v_2 = 0$ of the neutral.[7] The propensity rules of Simons indicate that such a crossing would result in rapid electron detachment from any anion states above the detachment threshold.[32]

None of these possibilities is entirely satisfactory. Thus, the identity of a component with $\tau = 14$ ms remains unclear, and the discrepancy between the <u>ab initio</u> results and the experimental data is unresolved.

Concluding Remarks

The best theoretical estimates of the radiative decay lifetimes of the bending mode of CH_2^- are 431 ms, 207 ms, 118 ms and 68 ms for the v_2 = 1, 2, 3 and 4 states respectively. From a fit to a three exponential model the measured values are $525^{+\infty}_{-230}$ ms, 70^{+50}_{-40} ms and 14^{+7}_{-7} ms. The first value is consistent with the v_2 = 1 theoretical lifetime but the remaining two are significantly shorter than predicted by theory. If the data are fit to a sum of four exponentials (assuming a geometric progression of lifetimes), we again find that the two shortest lifetimes are less than the theoretical values. Furthermore, a model using the four theoretically determined lifetimes fails to fit the data at times less than 20 ms. The theoretical results are consistent with the experimentally observed decay curve only if we postulate contributions to the photodetachment signal from an additional state of CH_2^- with a 15 ms lifetime, that is not a bending vibrational state (at least for the lowest rotational state of a vibrational state). However, alternative explanations for this fast decay, such as due to stretching vibrational states or highly excited ro-vibrational states, are not entirely consistent with our observations and calculations either. Thus, the identity of the τ = 14 ms component remains in doubt.

Experimental and theoretical studies of radiative decay lifetimes of vibrationally excited polyatomic molecules are very difficult, although many of the difficulties in this study are no doubt due to the anionic nature of CH_2^-. Consequently, in order to reach definitive assignments of the radiative decay lifetimes of CH_2^-, more exact theoretical methods will probably be needed and experimentally better signal to noise ratio over a longer time range is required. There are two main areas in which the ab initio determinations could possibly be improved. The first is the method used for determining the

electronic wave function or dipole moment surface. Ideally, one would like a large basis set (with f-functions on C and d-functions on H) coupled with a large MCSCF-CI. Secondly, coupling of all the vibrational motions would be preferable although it is not clear how large an effect this will produce. It is probably true, though, that the radiative decay lifetimes of the upper levels would be affected most. Finally, we would suggest that the best approach for definitive assignments of radiative decay lifetimes of polyatomic systems would seem to be the coupling of theory and experiment, because the experimental results alone do not always allow unique assignments to be made.

Acknowledgment

The authors thank Dr. P. R. Bunker for a copy of his SRB program and helpful correspondence. We also thank Professor W. C. Lineberger and Dr. D. G. Leopold for helpful discussions. This research was supported by the Director, Office of Energy Research, Office of Basic Energy Sciences, Chemical Sciences Division of the U.S. Department of Energy under Contract No. DE-AC03-76SF00098.

References

1. M. Okumura, L. I.-C. Yeh, D. Normand, J. J. H. van den Biesen, S. W. Bustamente, and Y. T. Lee, Tetrahedron 41, 1423 (1985).
2. R. R. Corderman and W. C. Lineberger, Ann. Rev. Phys. Chem. 30, 347 (1979).
3. B. K. Janousek and J. I. Brauman, Gas Phase Ion Chemistry, (Edited by M. T. Bowers), Vol. 2, p. 53. Academic Press, New York (1979).
4. P. C. Engelking, R. R. Corderman, J. J. Wendoloski, G. B. Ellison, S. V. ONeil, and W. C. Lineberger, J. Chem. Phys. 74, 5460 (1981).
5. A. R. W. McKellar, P. R. Bunker, T. J. Sears, K. M. Evenson, R. J. Saykally, and S. R. Langhoff, J. Chem. Phys. 79, 5251 (1983).
6. D. G. Leopold, K. K. Murray, A. E. Stevens Miller, and W. C. Lineberger, J. Chem. Phys. 83, 4849 (1985).
7. L. B. Harding and W. A. Goddard III, Chem. Phys. Lett. 55, 217 (1978).
8. P. R. Bunker and S. R. Langhoff, J. Mol. Spectrosc. 102, 204 (1983).
9. T. J. Lee and H. F. Schaefer, J. Chem. Phys. 83, 1784 (1985).
10. T. J. Lee, J. E. Rice and H. F. Schaefer, to be published.
11. H.-J. Werner, P. Rosmus, and E.-A. Reinsch, J. Chem. Phys. 79, 905 (1983).
12. P. Rosmus and H.-J. Werner, J. Chem. Phys. 80, 5085 (1984).
13. U. Mänz, A. Zilch, P. Rosmus, and H.-J. Werner, J. Chem. Phys. 84, 1683 (1986).
14. P. Botschwina, J. Mol. Spect. 117, 173 (1986).
15. P. Botschwina, Chem. Phys. Lett. 114, 58 (1985).
16. P. Botschwina, Habilitationsschrift
17. T. J. Lee, R. B. Remington, Y. Yamaguchi and H. F. Schaefer, J. Chem. Phys., to be published.

18. S. M. Adler-Golden, S. R. Langhoff, C. W. Bauschlicher, G. D. Carney, J. Chem. Phys. 83, 255 (1985).

19. P. R. Bunker and B. M. Landsberg, J. Mol. Spectrosc. 67, 374 (1977).

20. T. J. Sears and P. R. Bunker, J. Chem. Phys. 79, 5265 (1983). This SRB potential is derived from Ref. 4.

21. P. R. Bunker and T. J. Sears, J. Chem. Phys. 83, 4866 (1985). This SRB potential is derived from Ref. 6.

22. S. W. Bustamente, M. Okumura, D. Gerlich, H. S. Kwok, and L. R. Carlson, J. Chem. Phys. 86, 0000 (1987).

23. M. Okumura, L. I. Yeh, D. Normand and Y. T. Lee, J. Chem. Phys. 85, 1971 (1986).

24. F. B. van Duijneveldt, IBM Res. Dept. RJ945 (1971).

25. P. Saxe, D. J. Fox, H. F. Schaefer, and N. C. Handy, J. Chem. Phys. 77, 5584 (1982).

26. Y. Osamura, Y. Yamaguchi, and H. F. Schaefer, J. Chem. Phys. 77, 383 (1982).

27. J. E. Rice, R. D. Amos, N. C. Handy, T. J. Lee, and H. F. Schaefer, J. Chem. Phys. 85, 963 (1986).

28. G. H. F. Dierckson, B. D. Roos, A. J. Sadlej, Chem. Phys. 59, 29 (1981).

29. K. Raghavachari and J. A. Pople, Int. J. Quantum Chem. 20, 1067 (1981).

30. D. N. Neumark, K. R. Lykke, T. Andersen, and W. C. Lineberger, J. Chem. Phys. 83, 4364 (1985).

31. J. E. Delmore and A. D. Appelhans, J. Chem. Phys. 84, 6238 (1986).

32. J. Simons, J. Amer. Chem. Soc. 103, 3971 (1981).

Table I. Experimental lifetimes derived from fits of the data with sums of exponentials.

	Three Exponentials		Four Exponentials[a]	
v_2	Y_i	τ_i	Y_i	τ_i
1	2.6%	525 ms	3.1%	405 ms
2	3.2%	70	0.6%	135
3	3.0%	14	2.3%	45
4			2.8%	15

[a] τ_i were constrained to a geometric progression, with ratio $\tau_i/\tau_{i+1} = 3.0$.

Table II. CISD equilibrium geometries of CH_2^- using several basis sets. Bond lengths in Å and bond angles in degrees. See text for description of basis sets.

Basis Set	r_{C-H}	∠HCH
TZ + diffuse + 2P	1.116	102.5
TZ + 2 diffuse + 2P	1.116	102.5
TZ + diffuse + 3P'	1.116	102.6
TZ + diffuse + 3P	1.122	102.5

Table III. CISD total energies (Hartrees) and dipole moments (Debyes) of CH_2^- using several basis sets. Each dipole moment was evaluated as an energy derivative. See text for details concerning the basis sets.

Basis Set	Geometry of Calculation	E_{CISD}	μ
TZ + diffuse + 2P	Same method	-39.088974	1.98
TZ + 2 diffuse + 2P	Same method	-39.089076	2.00
TZ + diffuse + 3P'	Same method	-39.092463	1.97
TZ + diffuse + 3P	Same method	-39.089542	1.72
TZ + diffuse + 4P	TZ + diffuse + 3P	-39.089639	1.69
TZ + diffuse + 4P'	TZ + diffuse + 3P	-39.093362	1.76

Table IV. Radiative decay lifetimes (milliseconds) of the bending vibrational states of CH_2^-. The first column represents a purely ab initio value whereas the remaining columns coupled empirical potentials with an ab initio dipole moment function.[a]

v_2	Ab Initio[b]	Empirical[c]	Empirical[d]
1	431 (574)	471 (615)	491 (661)
2	207 (232)	231 (258)	231 (257)
3	118 (114)	134 (135)	129 (125)
4	68 (60)	82 (76)	75 (67)

[a]Values in parentheses were obtained with the TZ + diffuse + 3P basis while the others incorporated the TZ + diffuse + 4P basis.

[b]Purely ab initio values obtained with the appropriate basis. See text for details.

[c]See Ref. 20 for the first empirically derived SRB potential.

[d]See Ref. 21 for the second empirically derived SRB potential.

Table V. Bending vibrational energy levels determined from the semi-rigid-bender (SRB) wavefunctions. Units are cm^{-1}.

v_2	Ab Initio[a]		Sears and Bunker[b]	Bunker and Sears[c]
	TZ + diffuse + 3P	TZ + diffuse + 4P		
0	638	638	591	604
1	1934	1933	1789	1835
2	3212	3210	2970	3043
3	4466	4465	4131	4227
4	5689	5689	5272	5382

[a]This work.

[b]Reference 20.

[c]Reference 21.

Table VI. Transition moment matrix elements between the bending vibrational levels. Semi-rigid-bender (SRB) vibrational wavefunctions were coupled with the TZ diffuse + 4P dipole moment function.[a] The SRB wavefunctions were determined from both ab initio and empirically derived potential energy functions.

v_2	v_2'	Ab Initio	Empirical[b]	Empirical[c]
1	0	0.05835 (0.05050)	0.06277 (0.05493)	0.05908 (0.05090)
2	0	-0.01599 (-0.01890)	-0.01414 (-0.01758)	-0.01670 (-0.01981)
2	1	0.07271 (0.06057)	0.08226 (0.07051)	0.07436 (0.06170)
3	0	-0.00328 (-0.00335)	-0.00504 (-0.00554)	-0.00358 (-0.00367)
3	1	-0.03063 (-0.03569)	-0.02660 (-0.03205)	-0.03181 (-0.03711)
3	2	0.07561 (0.05839)	0.09301 (0.07634)	0.07854 (0.06057)
4	0	-0.00007 (-0.00001)	-0.00095 (-0.00068)	-0.00011 (0.00001)
4	1	-0.00614 (-0.00674)	-0.00950 (-0.01135)	-0.00666 (-0.00740)
4	2	-0.04873 (-0.05531)	-0.04147 (-0.04801)	-0.05034 (-0.05705)
4	3	0.06857 (0.04543)	0.09716 (0.07504)	0.07317 (0.04912)

[a]Values in parentheses are due to the TZ + diffuse + 3P basis.

[b]See reference 20.

[c]See reference 21.

Table VII. Einstein A coefficients for the coupling of bending vibrational levels. The Semi-rigid-bender (SRB) bending vibrational wavefunctions were coupled with the TZ + diffuse + 4P dipole moment function.[a] Both ab initio and empirical potential functions were used. Units are second^{-1}.

v_2	v_2'	Ab Initio	Empirical[b]	Empirical[c]
1	0	2.31969 (1.74133)	2.12396 (1.62650)	2.03709 (1.51203)
2	0	1.36463 (1.91045)	0.84336 (1.30459)	1.26854 (1.78534)
2	1	3.45704 (2.39981)	3.49127 (2.56480)	3.06030 (2.10721)
3	0	0.18950 (0.19707)	0.35379 (0.42703)	0.19078 (0.20053)
3	1	4.77557 (6.48085)	2.85097 (4.13962)	4.34464 (5.91491)
3	2	3.53832 (2.10750)	4.25278 (2.86484)	3.20985 (1.90933)
4	0	0.00022 (0.00000)	0.02924 (0.01493)	0.00042 (0.00000)
4	1	0.62710 (0.75423)	1.19563 (1.70773)	0.62006 (0.76694)
4	2	11.34029(14.59012)	6.58413 (8.82556)	10.17250(13.06543)
4	3	2.70566 (1.18553)	4.39718 (2.62302)	2.58848 (1.16645)

[a]Values in parantheses are due to the TZ + diffuse + 3P basis.

[b]See reference 20 for the empirically derived SRB potential.

[c]See reference 21 for the empirically erived SRB potential.

Figure Captions

Figure 1. Schematic of ion spectrometer.

Figure 2. Decay of the photodetachment signal at 4700 cm^{-1}. Curve is best fit of a triple exponential to the data, with lifetimes of 525 ms, 70 ms, and 14 ms. Lower plot shows detail of the first 160 ms of the upper plot.

Figure 3. Power dependence of the photodetachment signal at 4700 cm^{-1}, taken at two trapping times a) 1 ms and b) 30 ms.

Figure 4. Ab initio potential energy curves for CH_2^-. See text for details of the basis sets.

Figure 5. Ab initio dipole moment curves for the bending mode of CH_2^-. See text for details.

Figure 6. The ab initio optimium bond length of CH_2^- for various HCH angles. The TZ + diffuse + 3P basis was used. See text for details of this basis.

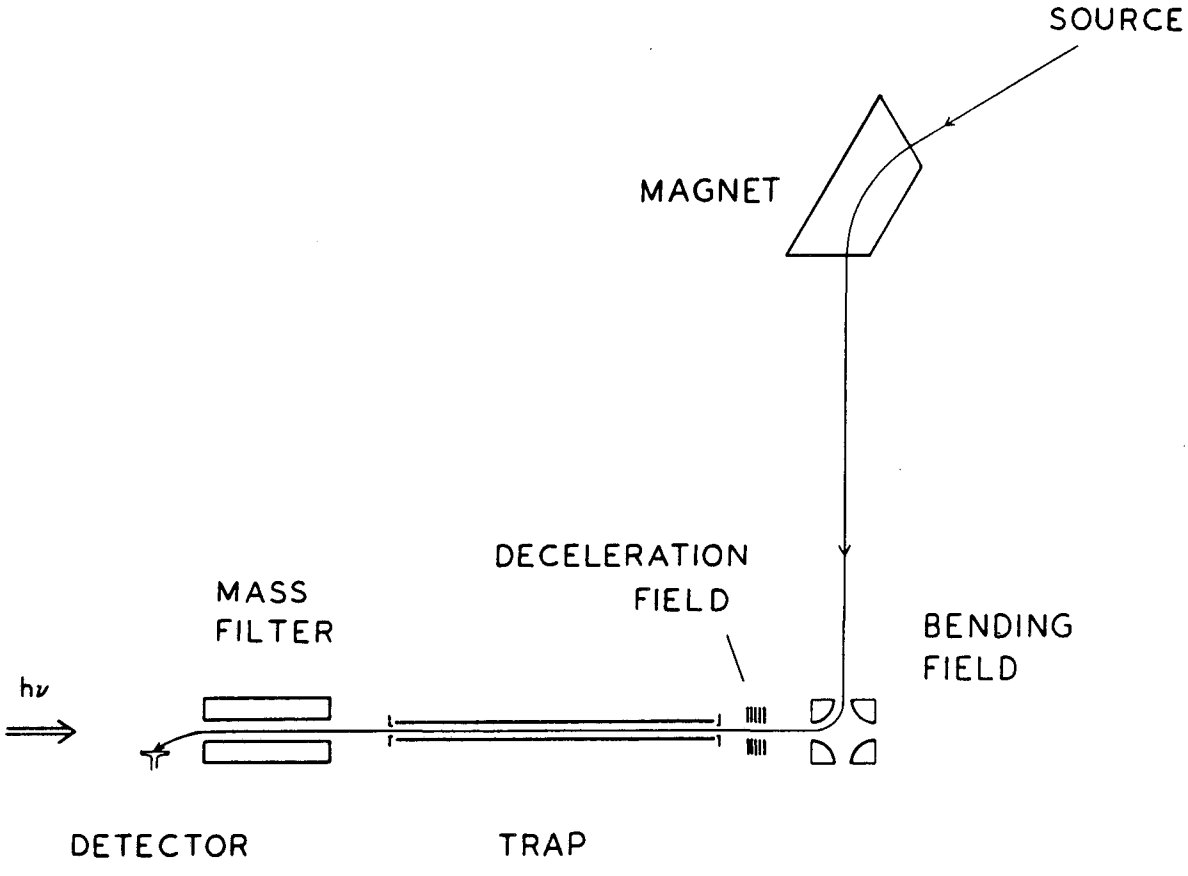
SOURCE
MAGNET
DECELERATION
FIELD
MASS
FILTER
BENDING
FIELD
hν
DETECTOR
TRAP

XBL 847-3011

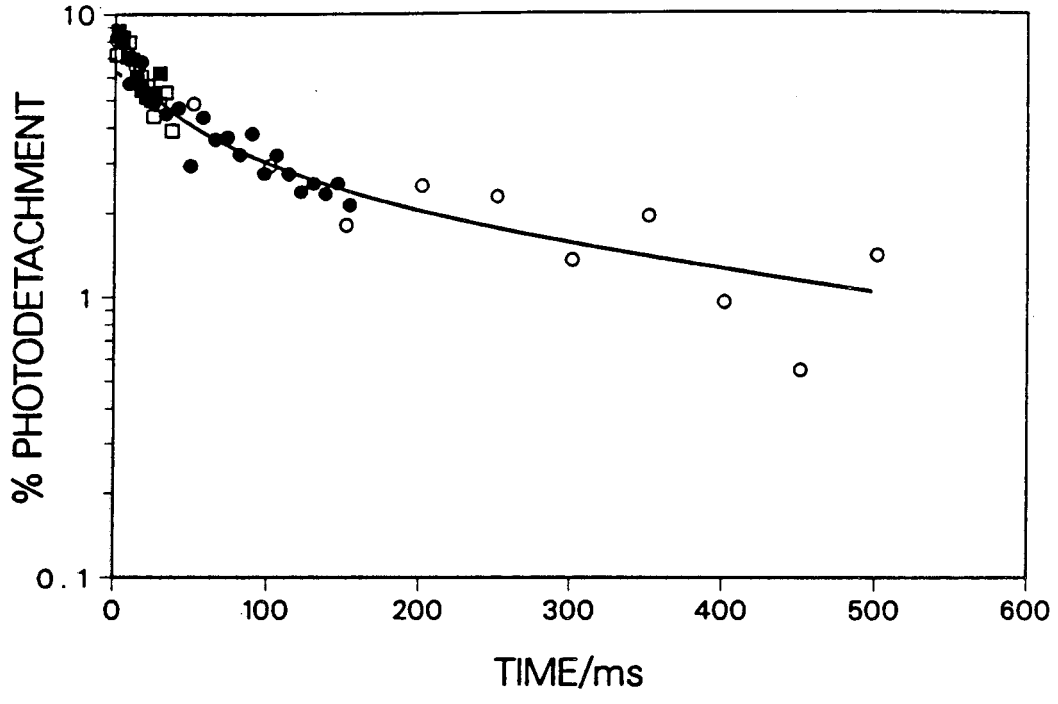

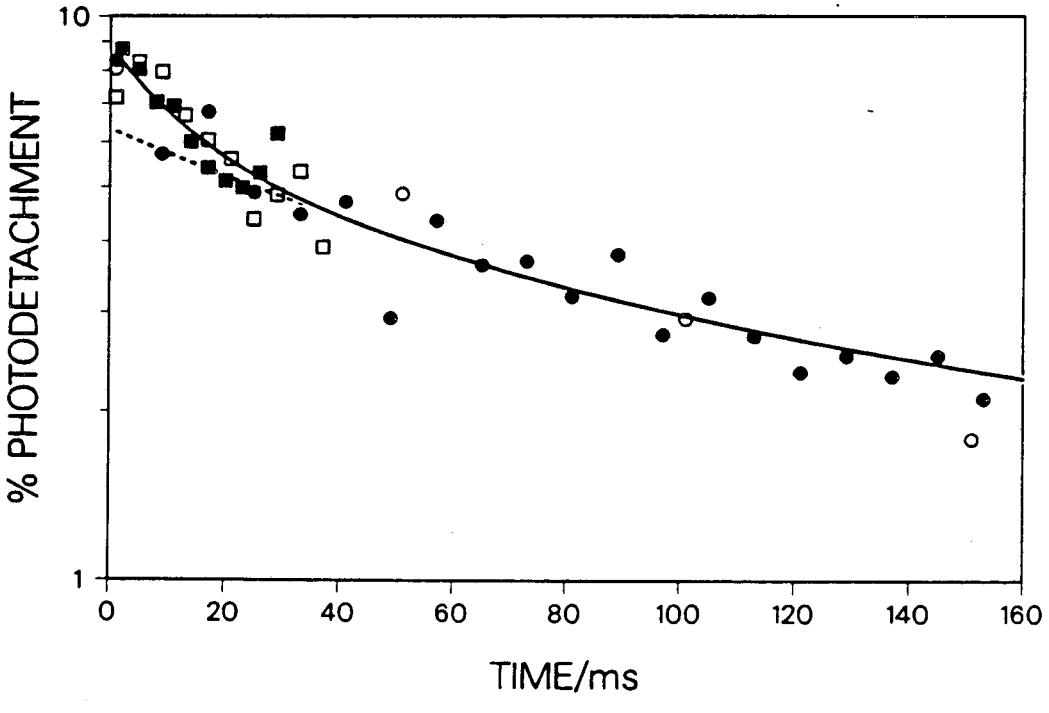

XBL 8610-3967

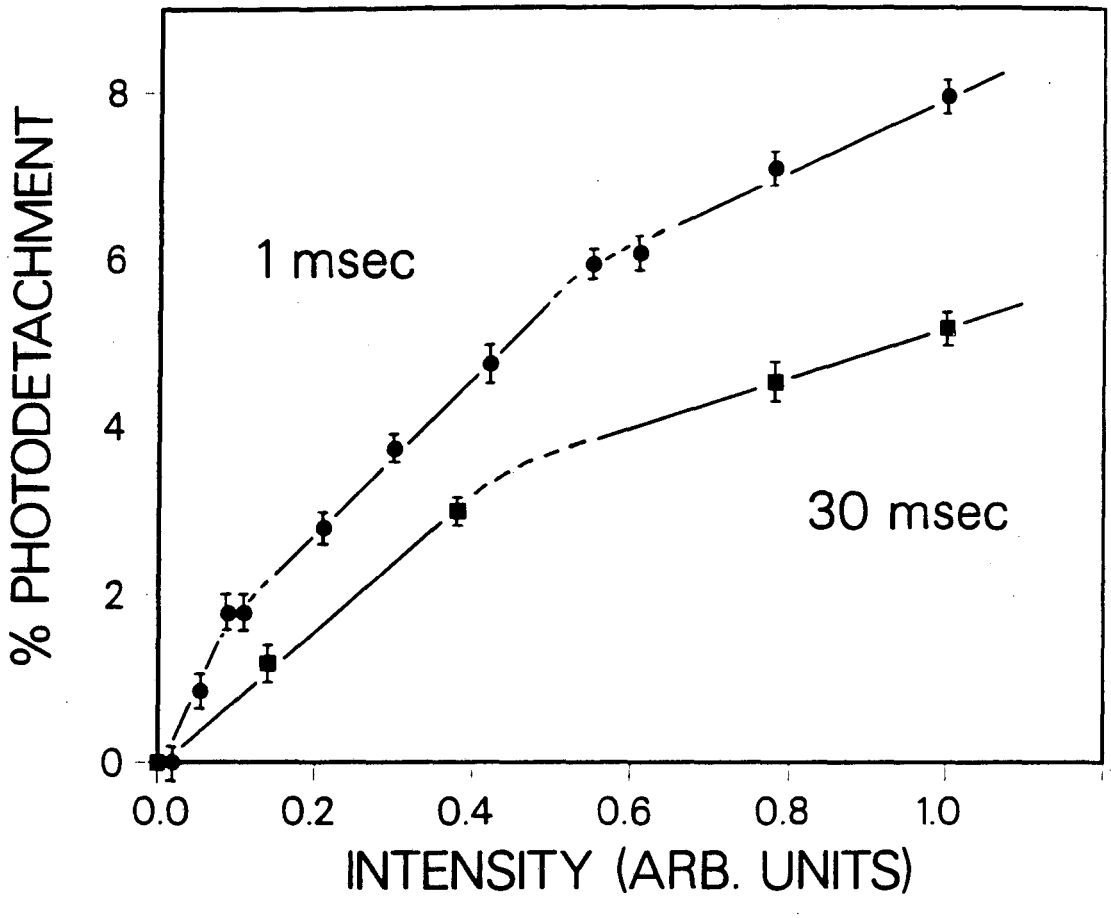
% PHOTODETACHMENT
8
6
4
2
0
1 msec
30 msec
0.0
0.2
0.4
0.6
0.8
1.0
INTENSITY (ARB. UNITS)

XBL 845-1707

POTENTIAL ENERGY FUNCTION OF CH_2^-

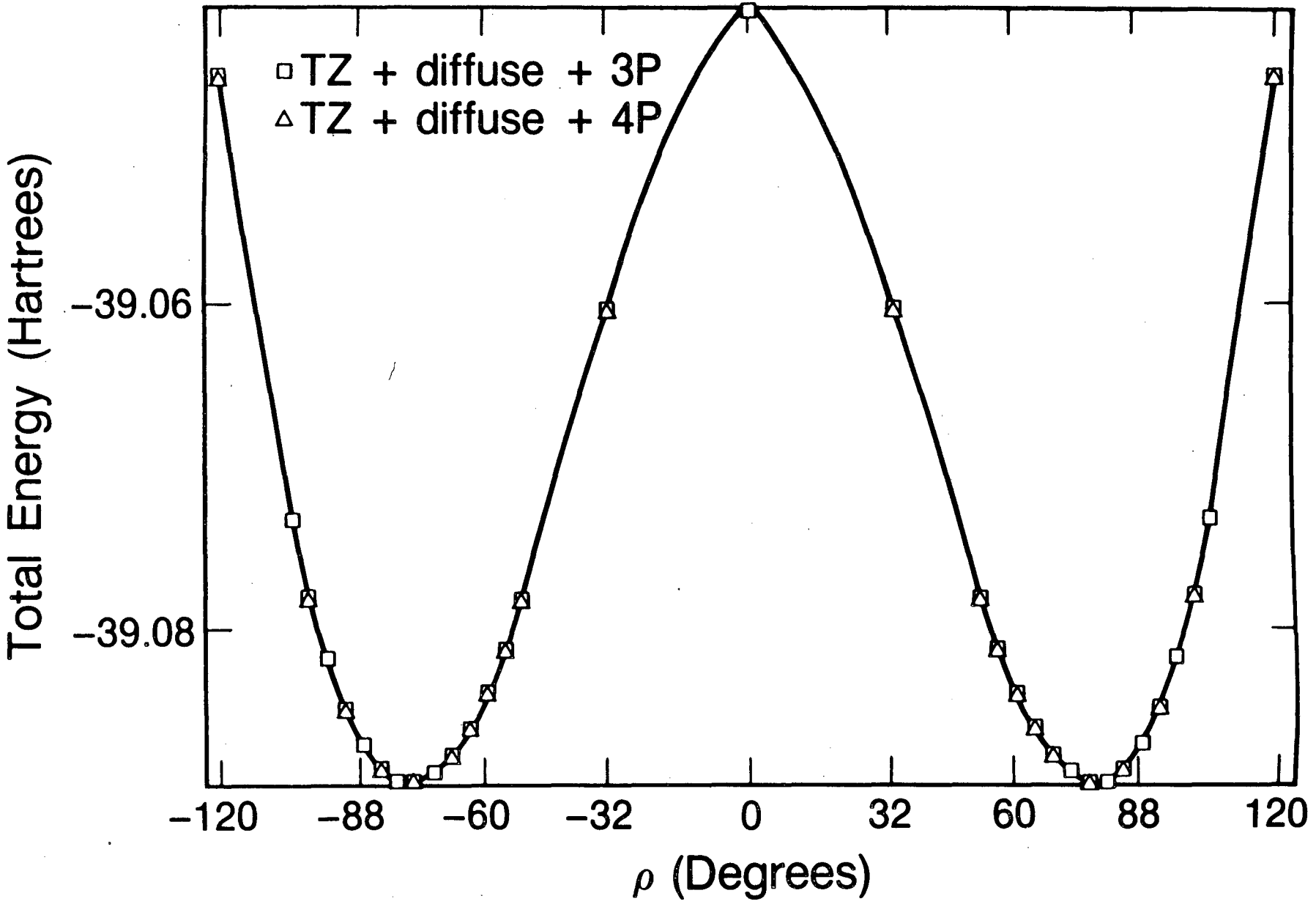

XBL 865-8773

DIPOLE MOMENT FUNCTION OF CH_2^-

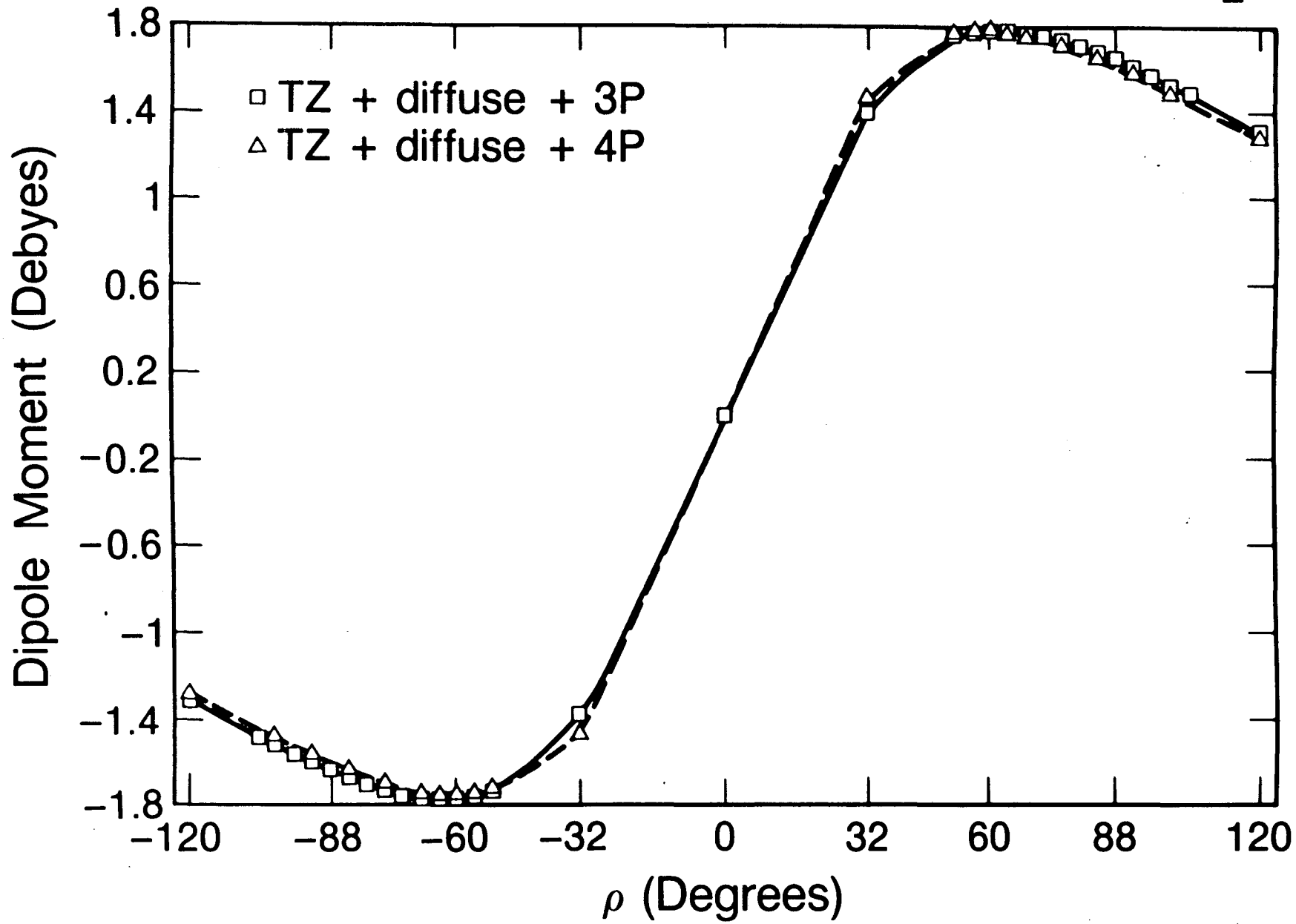

XBL 865-8774

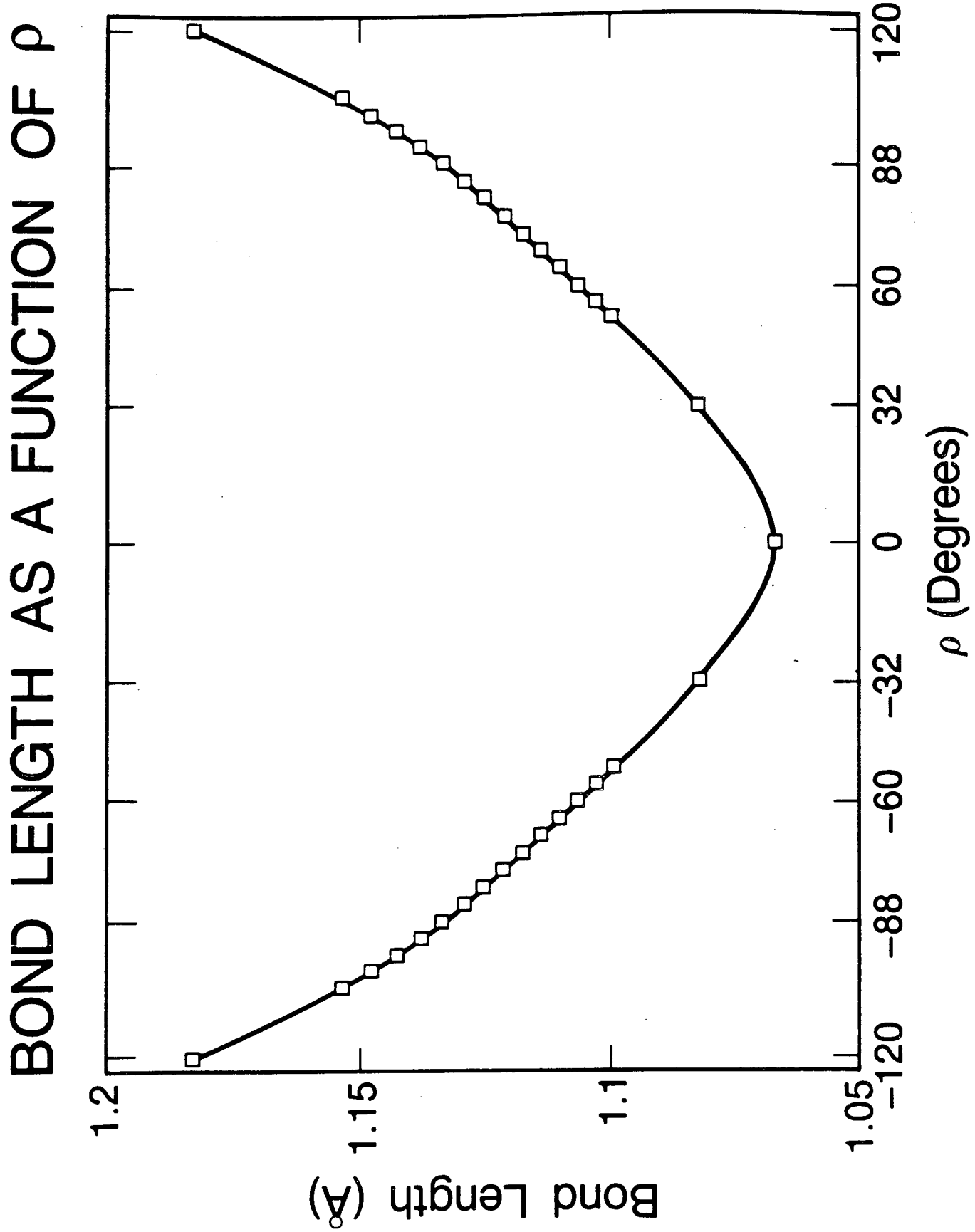
BOND LENGTH AS A FUNCTION OF ρ
Bond Length (Å)
1.2
1.15
1.1
1.05
−120
−88
−60
−32
0
32
60
88
120
ρ (Degrees)

XBL 865-8772

LAWRENCE BERKELEY LABORATORY
TECHNICAL INFORMATION DEPARTMENT
UNIVERSITY OF CALIFORNIA
BERKELEY, CALIFORNIA 94720